Dominant Thermodynamic Role of the Third Independent Receptor Binding Site in the Receptor-Associated Protein RAP†

Olav M. Andersen,‡ Frederick P. Schwarz,§ Edward Eisenstein,§ Christian Jacobsen,|| Søren K. Moestrup,|| Michael Etzerodt,‡ and Hans C. Thøgersen*,‡

Laboratory of Gene Expression, Department of Molecular and Structural Biology, and Department of Medical Biochemistry, University of Aarhus, Aarhus, Denmark, and Center for Advanced Research in Biotechnology, National Institute of Standards and Technology, Rockville, Maryland 20850

Received May 23, 2001; Revised Manuscript Received September 18, 2001

ABSTRACT: The 39 kDa receptor-associated protein (RAP) is a three-domain escort protein in the secretory pathway for several members of the low-density lipoprotein receptor (LDLR) family of endocytic receptors, including the LDLR-related protein (LRP). The minimal functional unit of LRP required for efficient binding to RAP is composed of complement-type repeat (CR)-domain pairs, located in clusters on the extracellular part of LRP. Here we investigate the binding of full-length RAP and isolated RAP domains 1−3 to an ubiquitin-fused CR-domain pair consisting of the fifth and sixth CR domains of LRP (U-CR56). As shown by isothermal titration calorimetric analysis of simple RAP domains as well as adjoined RAP domains, all three RAP domains bind to this CR-domain pair in a noncooperative way. The binding of U-CR56 to RAP domains 1 and 2 is (at room temperature) enthalpically driven with an entropy penalty ($K_D = 2.77 \times 10^{-6}$ M and 1.85×10^{-5} M, respectively), whereas RAP domain 3 binds with a substantially lower enthalpy, but is favored due to a positive entropic contribution ($K_D = 1.71 \times 10^{-7}$ M). The heat capacity change for complex formation between RAP domain 1 and the CR-domain pair is -1.65 kJ K^{-1} mol^{-1}. There is an indication of a conformational change in RAP domain 3 upon binding in the surface plasmon resonance analysis of the interaction. The different mechanisms of binding to RAP domains 1 and 3 are further substantiated by the different effects on binding of mutations of the Asp and Trp residues in the LRP CR5 or CR6 domains, which are important for the recognition of several ligands.

A large number of proteins are known to be endocytosed by members of the low-density lipoprotein receptor (LDLR)[1] family, including the LDLR-related protein (LRP) (*1*), the very low-density lipoprotein receptor (VLDLR) (*2*), the apoE receptor 2 (apoER2) (*3*), megalin, sorLA (LR11) (*4*, *5*), LRP5 (*6*−*8*), and LRP6 (*9*). These multidomain receptors contain clusters of complement-type repeat (CR) domains at various multiplicities; e.g., the canonical LDLR contains a single cluster with seven CR domains, whereas LRP comprises 31 CR domains located in four clusters of 2, 8, 10, and 11 CR domains, counting from the amino-terminal end. The CR domain consists of approximately 40 residues, including six strictly conserved Cys residues, linked to form three invariable disulfide bridges that connect Cys^{I} and Cys^{III}, Cys^{II} and Cys^{V}, and Cys^{IV} and Cys^{VI}. The three-dimensional structures of single CR domains 1, 2, 5, and 6 in LDLR and CR domains 3 and 8 in LRP show the burial of a Ca^{2+} ion in each domain, coordinated in part by negatively charged residues (*10*−*15*). Structural analysis of CR-domain pairs from LDLR has provided evidence that the CR domains are connected by a flexible linker providing no interdomain contacts (*16*−*19*).

A large number of ligands, such as proteinase−proteinase inhibitor complexes, lipase- and lipoprotein-containing particles, minor group viruses, and the amyloid protein precursor, have been reported to enter the cell via LRP-mediated endocytosis (for a recent review, see ref *20*).

The many structurally unrelated protein ligands exhibit a complex cross-inhibition pattern, suggesting that LRP contains a large number of different binding sites, where the binding specificity is determined by individual CR domains either alone or in combination with multiple homologous domains. Thermodynamic studies of these protein−protein interactions are helpful in understanding the forces that determine the affinity and selectivity of ligand recognition among the highly similar CR domains.

The receptor-associated protein (RAP) is a 323-amino acid residue protein, initially discovered as a protein that co-

† This work was supported by Grant 9901730 from the Danish National Science Research Council. O.M.A. gratefully acknowledges funding from NIST for travel expenses to the United States to perform the ITC measurements at CARB.

* To whom correspondence should be addressed. E-mail: hct@biobase.dk. Fax: +45 86 18 01 85. Telephone: +45 86 20 20 00.

‡ Laboratory of Gene Expression, Department of Molecular and Structural Biology, University of Aarhus.

§ National Institute of Standards and Technology.

|| Department of Medical Biochemistry, University of Aarhus.

[1] Abbreviations: RAP, receptor-associated protein; RAPd1, RAP residues 18−112; RAPd2, RAP residues 113−215; RAPd3, RAP residues 216−323; LDLR, low-density lipoprotein receptor; LRP, LDLR-related protein; ITC, isothermal titration calorimetry; CR, complement-type repeat; U-CR*xy*, ubiquitin-fused CR-domain pair from LRP CR cluster II; SPR, surface plasmon resonance. Certain commercial materials, instruments, and equipment are identified in this paper to specify the experimental procedure as completely as possible. In no case does such identification imply a recommendation or endorsement by the National Institute of Standards and Technology, nor does it imply that the materials, instruments, or equipment identified is necessarily the best available for the purpose.

10.1021/bi0110692 CCC: $20.00
Published on Web 11/22/2001

purifies with LRP from human placenta (*21*, *22*). RAP is a key protein in the endoplasmic reticulum and the Golgi compartments of the cell interior (*23*), where it serves as a molecular chaperone assisting processing of LRP (*24*−*26*). From a limited triplicate sequence homology of the primary structure (*27*), RAP has been suggested to contain three domains, RAPd1 (RAP residues 18−112), RAPd2 (residues 113−215), and RAPd3 (residues 216−323), plus an amino-terminal 17-residue tail, as suggested by Ellgaard et al. (*28*). An alternative three-domain dissection has been proposed by Bu and colleagues (RAPd1 comprising residues 1−100, RAPd2 comprising residues 101−200, and RAPd3 comprising residues 201−323) (*23*, *27*), and recently, a four-domain composition has also been proposed (*29*). All three RAP domains, as defined by Ellgaard, are able to bind immobilized LRP, with the following affinity order: RAPd3 > RAPd1 > RAPd2 [as analyzed by surface plasmon resonance (SPR) analysis (*30*)]. Furthermore, whereas domain 2 is a poor inhibitor of ^{125}I-labeled RAP binding to LRP, domain pairs of RAP containing RAPd1 and RAPd2, and RAPd2 and RAPd3, are far better inhibitors of full-length RAP binding to LRP as are the single domains RAPd1 and RAPd3, which suggest that each domain contains an LRP recognition site (*28*).

RAP is also able to inhibit binding and/or uptake of all known LRP ligands (*31*−*36*). The mechanism by which RAP universally inhibits ligand binding of LRP has been debated, and two mutually, nonexclusive models have been suggested. The demonstration of several independent RAP binding sites (*37*−*39*) on each LRP molecule suggests that the multiple binding sites overlap with individual binding sites for other LRP ligands, allowing RAP to either competitively or sterically hinder the binding of these LRP ligands. The alternative model for RAP inhibition of ligand binding suggests that upon binding to LRP, RAP induces a conformational change, which prevents further ligand binding (*40*, *41*). However, it is possible that a combination of conformation changes in LRP and steric hindrance is in fact the basis for the antagonist function of RAP (reviewed in refs *42* and *43*). We have demonstrated that the minimal functional units of LRP that are able to recognize isolated RAP domains are pairs of CR domains (*39*). Recently, it was shown that one RAP molecule can link at least two clusters of CR domains simultaneously, suggesting that more than one receptor-binding site in RAP can be engaged at the same time (*41*). To elucidate the mechanism of RAP inhibition, a thermodynamic characterization of the interaction between the ubiquitin-fused CR56-domain pair of LRP (U-CR56) and full-length RAP as well as isolated RAP domains was undertaken using isothermal titration calorimetry (ITC). The following reactions were characterized in terms of the dissociation constant (K_D) and changes in the free energy (ΔG_b°), enthalpy (ΔH_b°), and entropy (ΔS_b°).

$$\text{RAPd1} + \text{U-CR56} \leftrightarrow \text{RAPd1·U-CR56} \quad \text{(I)}$$

$$\text{RAPd2} + \text{U-CR56} \leftrightarrow \text{RAPd2·U-CR56} \quad \text{(II)}$$

$$\text{RAPd3} + \text{U-CR56} \leftrightarrow \text{RAPd3·U-CR56} \quad \text{(III)}$$

$$\text{RAP} + 3\text{U-CR56} \leftrightarrow [\text{RAP·U-CR56}] + 2\text{U-CR56} \leftrightarrow [\text{RAP·(U-CR56)}_2] + \text{U-CR56} \leftrightarrow \text{RAP·(U-CR56)}_3 \quad \text{(IV)}$$

The effect of mutations in U-CR56 on the thermodynamics of the binding reactions was also investigated.

EXPERIMENTAL PROCEDURES

Expression, Refolding, and Processing of Recombinant Proteins. The U-CR56 fusion protein containing the wild-type amino acid sequence and U-CR56 derivatives with single-residue substitutions were expressed in *Escherichia coli* AG1 cells, in vitro refolded, and purified, partly using RAP domain affinity chromatography, as described previously (*39*, *44*).

RAP (*34*), RAPd1, RAPd2 (*28*), and RAPd3 (*39*) were also obtained from *E. coli*, as previously described. The concentration of each protein was calculated using the extinction coefficients calculated using the ExPaSy server facility as described previously (*39*).

Isothermal Titration Calorimetry Binding Analysis. All titrations were performed with a VP ITC from MicroCal Inc. (Northampton, MA) (*45*). Titrations were performed into a cell with a volume of 1.4019 mL with injections of either 10 or 12 μL from a syringe being stirred at 310 rpm. All protein samples were in 140 mM NaCl, 2 mM $CaCl_2$, and 10 mM HEPES (pH 7.4), and samples were degassed by stirring under vacuum prior to use. The heat of dilution was determined to be negligible in separate titrations of ligand solutions into buffer solutions. Binding isotherms were fitted using ORIGIN version 5.0 from MicroCal Inc. utilizing either a one-site or a two-site binding model. The binding model for a single set of sites was used to fit the incremental heat of the ith injection [$\Delta Q(i)$] of the total heat, Q_t, to the total titrant concentration, L_t, according to the following equations (*45*)

$$Q_t = nC_t\Delta H_b^\circ V(1 + L_t/(nC_t) + 1/(nK_AC_t) - \{[1 + L_t/(nC_t) + 1/(nK_AC_t)]^2 - 4L_t/nC_t\}^{1/2})/2 \quad (1)$$

$$\Delta Q_i = Q(i) + dV_i/\{2V[Q(i) + Q(i-1)]\} - Q(i-1) \quad (2)$$

where K_A is the association constant, n is the stoichiometry of the binding reaction, C_t is the total protein concentration in the sample cell, V is the cell volume, and dV_i is the volume of titrant added to the solution. For ligand binding to two sets of sites, the fraction of protein bound with one ligand, F_1, where [L] is the free ligand concentration, is

$$F_1 = (K_1[\text{L}])/(1 + K_1[\text{L}] + K_1K_2[\text{L}]^2) \quad (3)$$

and the fraction of protein bound with two ligands, F_2, is

$$F_2 = (K_1K_2[\text{L}]^2)/(1 + K_1[\text{L}] + K_1K_2[\text{L}]^2) \quad (4)$$

so that eq 1 becomes

$$Q_t = C_tV[F_1\Delta H_b^\circ{}_1 + F_2(\Delta H_b^\circ{}_1 + \Delta H_b^\circ{}_2)] \quad (5)$$

Then the heat released per addition of titrant is fitted to eq 2 using the four parameters K_1, K_2, $\Delta H_b^\circ{}_1$, and $\Delta H_b^\circ{}_2$, where K_i and $\Delta H_b^\circ{}_i$ are the association constant and the enthalpy of binding for the two binding reactions. The thermodynamic quantities, ΔG_b° and ΔS_b°, were determined using the

fundamental equation of thermodynamics

$$\Delta G_b^\circ = \Delta H_b^\circ - T\Delta S_b^\circ \quad (6)$$

where

$$\Delta G_b^\circ = -RT \ln(K_A) \quad (7)$$

and $R = 8.314$ J mol^{-1} K^{-1} and T is the absolute temperature.

Standard deviations of the parameters K_A (s_{K_A}), ΔH_b° ($s_{\Delta H}$), and n were directly obtained from the iterative fitting procedure using ORIGIN, and the standard deviations for ΔG_b° ($s_{\Delta G}$), ΔS_b° ($s_{\Delta S}$), and K_D (s_{K_D}) were calculated using the following equations

$$s_{\Delta G} = RT(s_{K_A}/K_A) \quad (8)$$

$$s_{\Delta S} = (s_{\Delta H}{}^2 + s_{\Delta G}{}^2)^{1/2} \quad (9)$$

$$s_{K_D} = s_{K_A}/K_A{}^2 \quad (10)$$

The heat capacity changes for complex formation, ΔC_p, were determined from a linear plot of ΔH_b° versus T ($\Delta C_p = \delta\Delta H_b^\circ/\delta T$) for the titration of U-CR56 with RAPd1 at 298, 308, and 318 K.

Surface Plasmon Resonance Binding Analysis. BIAcore type CM5 sensor chips (Biosensor, Uppsala, Sweden) were activated with a 1:1 mixture of 0.2 M *N*-ethyl-*N*-(3-dimethylaminopropyl)carbodiimide and 0.05 M *N*-hydroxysuccinimide in water according to the manufacturer, prior to immobilization of RAP, RAPd1, and RAPd3 [proteins were in 25 mM sodium acetate (pH 5.0) and 150 mM NaCl] which were injected at concentrations of 5, 30, and 15 μg/mL, respectively, resulting in total protein coupling densities of 165, 14, and 185 fmol/mm^2, respectively. The biosensor chips were capped by exposure to 1 M ethanolamine (pH 8.5). The binding analysis was conducted with U-CR56 in running buffer [150 mM NaCl, 5 mM $CaCl_2$, 10 mM HEPES (pH 7.4), and 0.005% Tween 20] at 20, 50, 100, 200, 500, 1000, and 5000 nM, and a flow rate of 5 μL/min. Regeneration of the biosensor chip was performed using 1.6 M glycine-HCl (pH 3.1). Kinetic parameters were determined using the BIAevaluation program version 3.1 (BIAcore, Uppsala, Sweden), where sensorgrams were fitted to a two-state reaction involving a conformational change:

$$A + B \underset{k_{d1}}{\overset{k_{a1}}{\rightleftharpoons}} [AB] \underset{k_{d2}}{\overset{k_{a2}}{\rightleftharpoons}} [AB]^* \quad (11)$$

The equilibrium constants of the individual steps are

$$K_{a1} = k_{a1}/k_{d1} \quad (12)$$

$$K_{a2} = k_{a2}/k_{d2} \quad (13)$$

and the overall equilibrium binding constant, K_A, is calculated as (*46*)

$$K_A = K_{a1}(1 + K_{a2}) \quad (14)$$

RESULTS

The titration of RAPd1 into a solution of U-CR56wt and vice versa generated nearly identical thermograms, as shown in panels A and D of Figure 1, respectively. The binding isotherms were determined by fitting the data to the single set of sites binding model. The thermodynamic parameters that are obtained are listed in Table 1. The entropy penalty $T\Delta S_b^\circ$ equaled -15.0 kJ mol^{-1} but was compensated by a favorable enthalpy ($\Delta H_b^\circ = -46.7$ kJ mol^{-1}). Similar results were obtained for the interaction between RAPd2 and U-CR56, though with an ~7-fold lower affinity ($T\Delta S_b^\circ = -39.4$ kJ mol^{-1}, $\Delta H_b^\circ = -66.5$ kJ mol^{-1}). Since the affinity of binding of RAPd2 to U-CR56 is rather low, the stoichiometry was fixed at 1 throughout the fitting to obtain accurate values for the binding enthalpy and affinity.

The titration of RAPd3 into U-CR56wt (Figure 1C) exhibited an ~16-fold higher affinity compared to the RAPd1 binding reaction but with a much less favorable enthalpy ($\Delta H_b^\circ = -22.8$ kJ mol^{-1}) and driven partly by a positive entropy contribution ($T\Delta S_b^\circ = 15.9$ kJ mol^{-1}). The reverse binding analysis, titrating U-CR56wt into RAPd3 (Figure 1F), yielded a binding isotherm which can only be accurately fitted using a two set of sites model with a stoichiometry of 0.15 for the high-affinity binding reaction and a stoichiometry of 0.93 for the second set of sites, which yielded thermodynamic parameters similar to those determined for the reverse titration. The level of high-affinity binding was 9×10^{-9} M, near the lower limit for K_D ITC analysis (*45*). However, the second part of the binding isotherm was fitted with similar parameters as in the opposite titration experiment, and we conclude that these parameters represent formation of a complex of RAPd3 and U-CR56.

The formation of a complex of full-length RAP and U-CR56wt was also analyzed by ITC, demonstrating a high-affinity binding reaction when RAP was titrated into a solution containing U-CR56 (Figure 2A) with a stoichiometry of 0.3, strongly suggestive of a concurrent binding of U-CR56 to all three RAP domains. To demonstrate the association of CR-domain pairs with each RAP domain, we also titrated U-CR56 into a RAP solution at different concentrations (Figure 2B,C). These binding isotherms show at least a two set of sites binding mechanism, but given the demonstrated stoichiometry of 0.3 in the reverse experiment, we speculated whether all three sites indeed could be associated with U-CR56. Therefore, we simulated the sequential binding using the thermodynamic parameters determined from the binding of isolated RAP domains from either of the two binding sites with the highest affinity (RAPd1 and RAPd3) or for all three binding sites. Clearly, the inclusion of the parameters for the interaction between RAPd2 and U-CR56 significantly improved the fit of the simulated binding curve to the measured ITC data as shown in Figure 2, again strongly supportive of the concurrent association of one CR-domain pair with each of the three RAP domains. Also, the titration of RAP into U-CR56 was simulated with the actually measured binding parameters, assuming that the three sets of sites are noninteracting, and the curve that was created showed good agreement with the observed binding data. The fits are shown in Figure 2, and a data summary is presented in Figure 3.

We also tested variants of RAPd1 and RAPd3, truncated at the carboxyl-terminal ends, to comprise residues 18−97 and 219−309, respectively, and observed a significant decrease in affinity for U-CR56 (not shown).

To further characterize the interaction between U-CR56wt and one of the isolated RAP domains, the titration of RAPd1

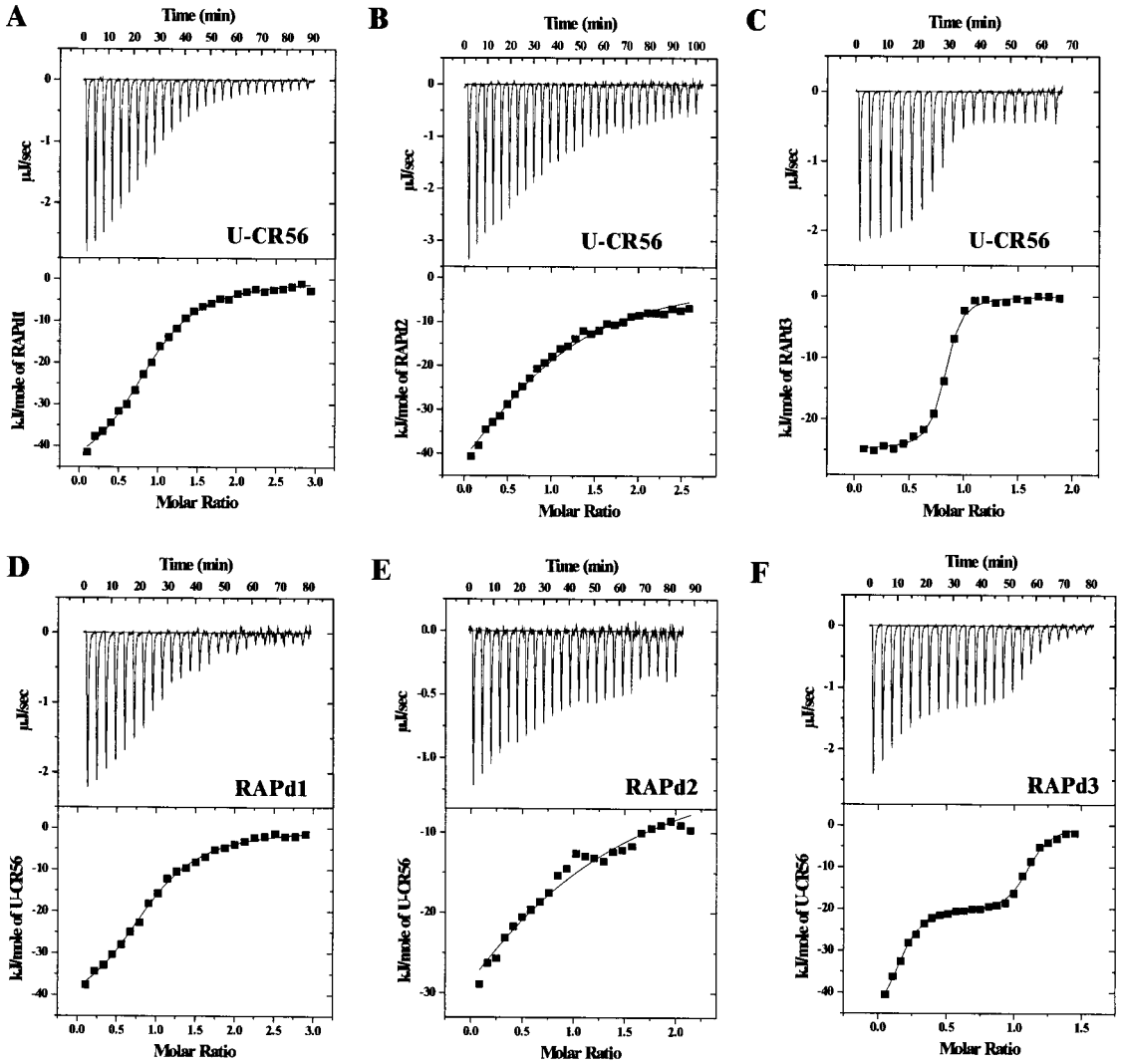

FIGURE 1: Representative thermograms and binding isotherms from the ITC analysis of the interactions between U-CR56 and RAPd1, RAPd2, and RAPd3. Panels A−C show the titration of RAPd1 (0.2290 mM), RAPd2 (0.3060 mM), and RAPd3 (0.2303 mM) into 0.01644, 0.0270, and 0.01869 mM U-CR56wt, respectively. Panels D−F show the reverse titrations of U-CR56 at concentrations of 0.1958, 0.1280, and 0.1958 mM into RAPd1 (0.01527 mM), RAPd2 (0.0135 mM), and RAPd3 (0.0306 mM), respectively. The solid lines correspond to the best fits to the data by a nonlinear least-squares regression algorithm (ORIGIN version 5.0), and the calculated thermodynamic parameters are listed in Table 1.

Table 1: Thermodynamic Parameters for the Interaction between U-CR56 and RAPd1, RAPd2, RAPd3, and RAP

	K_D (M)	$\Delta G_b°$ (kJ mol^{-1})	$\Delta H_b°$ (kJ mol^{-1})	$T\Delta S_b°$ (kJ mol^{-1})	stoichiometry
RAPd1 → U-CR56wt	$(2.65 \pm 0.17) \times 10^{-6}$	-31.8 ± 0.2	-48.1 ± 0.9	-16.3 ± 0.9	0.91 ± 0.01
U-CR56wt → RAPd1	$(2.89 \pm 0.20) \times 10^{-6}$	-31.6 ± 0.2	-45.3 ± 1.0	-13.7 ± 1.2	0.91 ± 0.01
RAPd2 → U-CR56wt	$(1.67 \pm 0.15) \times 10^{-5}$	-27.3 ± 0.2	-63.4 ± 2.1	-36.1 ± 2.1	1
U-CR56wt → RAPd2	$(2.02 \pm 0.24) \times 10^{-5}$	-26.8 ± 0.3	-69.6 ± 4.1	-42.8 ± 4.1	1
RAPd3 → U-CR56wt	$(1.26 \pm 0.16) \times 10^{-7}$	-39.4 ± 0.3	-24.9 ± 0.2	14.5 ± 0.4	0.79 ± 0.00
U-CR56wt → RAPd3					
i	$(9.08 \pm 2.31) \times 10^{-9}$	-45.9 ± 0.6	-47.0 ± 2.8	-1.1 ± 2.9	0.15 ± 0.01
ii	$(2.16 \pm 0.37) \times 10^{-7}$	-38.0 ± 0.4	-20.7 ± 0.5	17.3 ± 0.6	0.93 ± 0.01
RAP → U-CR56wt	$(7.84 \pm 0.70) \times 10^{-7}$	-34.8 ± 0.2	-124.6 ± 1.7	-89.7 ± 1.7	0.30 ± 0.003

into U-CR56wt was performed at 35 and 45 °C. The binding isotherms were fitted as for 25 °C, and the thermodynamic parameters that were calculated are listed in Table 2. The formation of a complex of RAPd1 and U-CR56wt becomes increasingly enthalpically driven with increasing temperatures, showing a negative ΔC_p of -1.65 kJ K^{-1} mol^{-1} from the slope of the $\Delta H_b°$ versus temperature curve (Figure 4) that is characteristic of hydrophobic associations (*47*).

U-CR56 Single-Residue Mutant Derivative Binding Analysis. Previously, we have demonstrated a critical role in ligand recognition of two surface-exposed residues at identical positions in the primary structure of a CR domain, e.g., CR5 (Trp953^{CR5} and Asp958^{CR5}) and CR6 (Trp994^{CR6} and Asp999^{CR6}) in the CR56 domain pair. The mutants U-CR56W953S, U-CR56D958N, U-CR56W994S, and U-CR56D999N have been described previously (*39*, *44*). Together with the two mutant derivatives U-CR56R947Q and U-CR56R988Q, we investigated the binding of these residue derivatives to isolated RAP domains. The titration of RAPd1 (0.2290 mM) into U-CR56 mutant proteins

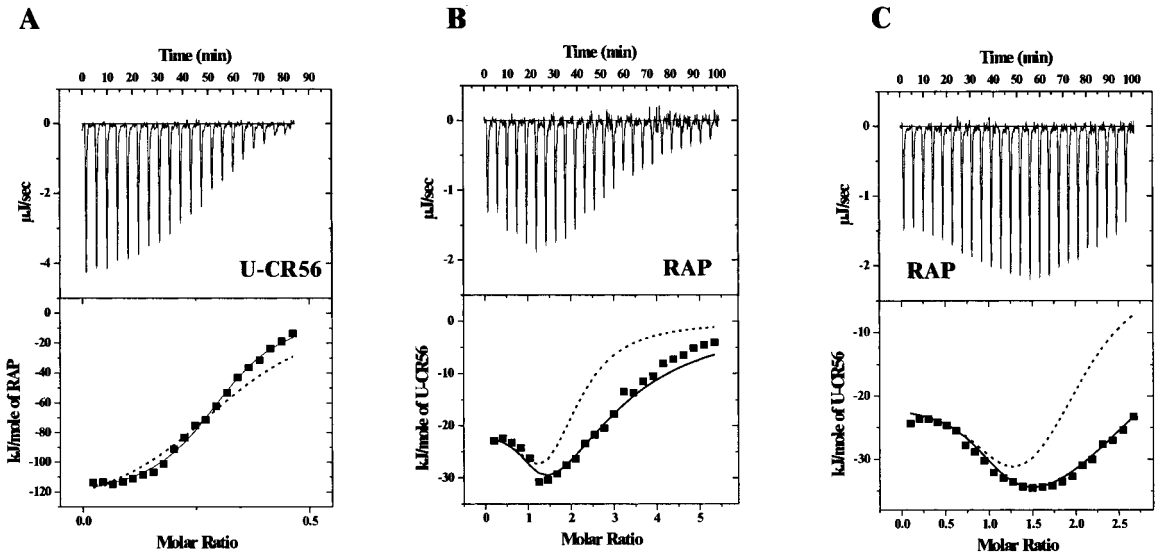

FIGURE 2: Analysis of multiple CR-domain pair binding to full-length RAP. Titration of either RAP (0.1246 mM) into U-CR56 (0.04895 mM) (A) or titration of U-CR56 (0.1958 mM) into RAP (0.0083 and 0.0166 mM in panels B and C, respectively). The solid line in panel A represents the best fit to the measured data assuming identical sites, whereas the dotted line is a simulation of the binding of three U-CR56 molecules concurrently and with no cooperativity to RAP with a stoichiometry of 0.33. Simulation of sequential binding to the obtained data shown in panels B and C, either assuming two sites with input of the measured thermodynamic parameters for only binding to RAPd3 and RAPd1 (dotted lines) or assuming that all three RAP domains can bind simultaneously (solid lines).

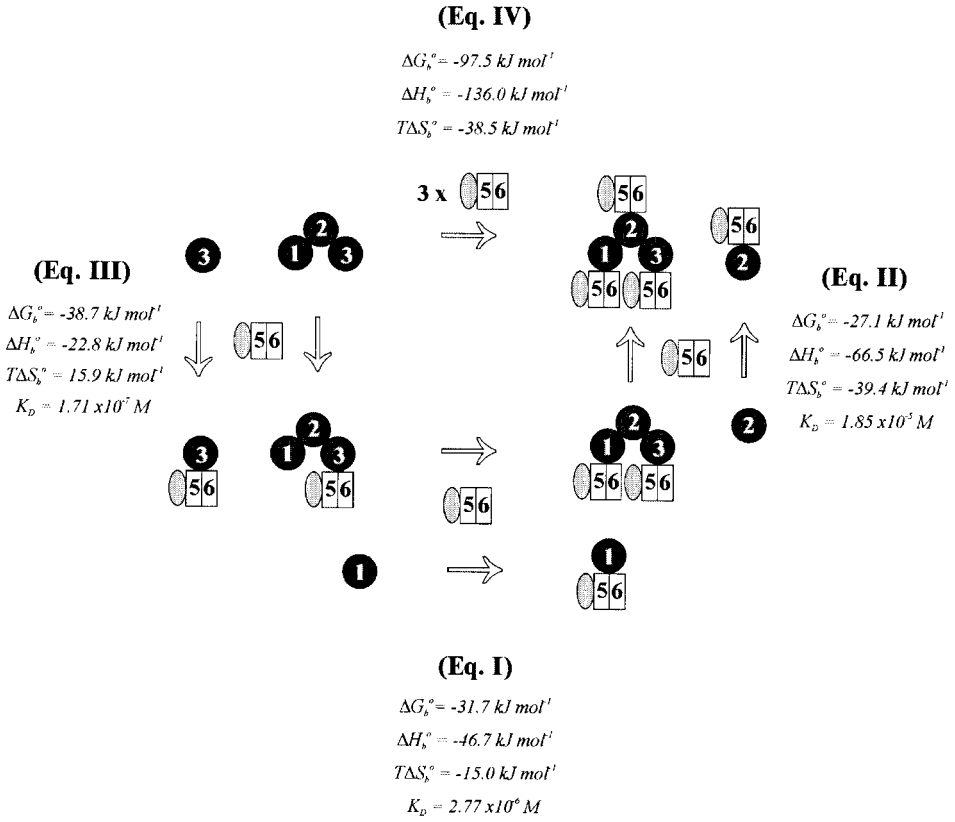

FIGURE 3: Schematic representation of the independent associations of each RAP domain with the CR domain pair. Thermodynamic parameters are the mean values obtained from the reverse titration experiments for binding of U-CR56 to RAPd3 (eq III), RAPd1 (eq I), and RAPd2 (eq II) as presented in the introductory section and shown in Figure 1 (listed in Table 1). Parameters for the association of full-length RAP with three U-CR56 molecules (eq IV) were calculated as the sum of the values for the three independent binding reactions, and used as input in the simulation of binding curves for the ternary complex formation and to compare with the actually measured binding data (Figure 2).

(0.0225 mM) showed that the two Asp → Asn and the two Trp → Ser substitutions eliminate binding to RAPd1, whereas the Arg → Gln substitutions do not (Table 3). The titration of RAPd3 (0.2303 mM) into the U-CR56 single-residue derivatives (0.0225 mM) also showed a decreased affinity for U-CR56D958N and U-CR56D999N, where the decrease is due to a less favorable entropy compared to that of U-CR56wt. The affinity of binding of RAPd3 to U-CR56W953S was also found to be decreased, compared to that for binding to U-CR56wt, but here complex formation

Table 2: Temperature Dependence of the Interaction between U-CR56 and RAPd1

	temp (°C)	K_D (M)	$\Delta G_b°$ (kJ mol^{-1})	$\Delta H_b°$ (kJ mol^{-1})	$T\Delta S_b°$ (kJ mol^{-1})	stoichiometry
RAPd1 → U-CR56wt	25	$(2.06 \pm 0.13) \times 10^{-6}$	-32.4 ± 0.2	-48.7 ± 0.7	-16.3 ± 0.7	0.83 ± 0.01
RAPd1 → U-CR56wt	35	$(5.67 \pm 0.24) \times 10^{-6}$	-30.9 ± 0.1	-64.1 ± 1.1	-33.1 ± 1.1	0.77 ± 0.01
RAPd1 → U-CR56wt	45	$(10.8 \pm 0.40) \times 10^{-6}$	-30.2 ± 0.1	-81.7 ± 2.1	-51.4 ± 2.1	0.71 ± 0.01

Table 3: Thermodynamic Parameters for the Interaction between U-CR56 Derivatives and RAP Derivatives

	K_D (M)	$\Delta G_b°$ (kJ mol^{-1})	$\Delta H_b°$ (kJ mol^{-1})	$T\Delta S_b°$ (kJ mol^{-1})	stoichiometry
RAPd1 → U-CR56wt	$(2.06 \pm 0.13) \times 10^{-6}$	-32.4 ± 0.2	-48.7 ± 0.7	-16.3 ± 0.7	0.83 ± 0.01
RAPd1 → U-CR56R947Q	$(2.20 \pm 0.20) \times 10^{-6}$	-32.3 ± 0.2	-51.4 ± 1.0	-19.1 ± 1.0	0.88 ± 0.01
RAPd1 → U-CR56W953S	NA[a]	NA[a]	NA[a]	NA[a]	NA[a]
RAPd1 → U-CR56D958N	NA[a]	NA[a]	NA[a]	NA[a]	NA[a]
RAPd1 → U-CR56R988Q	$(2.13 \pm 0.20) \times 10^{-6}$	-32.4 ± 0.2	-59.4 ± 1.3	-27.0 ± 1.3	0.80 ± 0.01
RAPd1 → U-CR56W994S	NA[a]	NA[a]	NA[a]	NA[a]	NA[a]
RAPd1 → U-CR56D999N	NA[a]	NA[a]	NA[a]	NA[a]	NA[a]
RAPd3 → U-CR56wt	$(2.77 \pm 0.51) \times 10^{-7}$	-37.4 ± 0.5	-28.7 ± 0.5	8.8 ± 0.7	0.83 ± 0.01
RAPd3 → U-CR56R947Q	$(2.17 \pm 0.36) \times 10^{-7}$	-38.0 ± 0.4	-32.0 ± 0.4	6.0 ± 0.6	0.91 ± 0.01
RAPd3 → U-CR56W953S	$(6.83 \pm 1.78) \times 10^{-6}$	-29.5 ± 0.6	-52.4 ± 3.5	-22.9 ± 3.6	1
RAPd3 → U-CR56D958N	$(2.42 \pm 0.23) \times 10^{-6}$	-32.0 ± 0.2	-32.0 ± 0.6	0.1 ± 0.6	0.99 ± 0.01
RAPd3 → U-CR56R988Q	$(1.36 \pm 0.19) \times 10^{-7}$	-39.2 ± 0.3	-38.6 ± 0.4	0.6 ± 0.5	0.83 ± 0.01
RAPd3 → U-CR56W994S	NA[a]	NA[a]	NA[a]	NA[a]	NA[a]
RAPd3 → U-CR56D999N	$(5.61 \pm 0.63) \times 10^{-6}$	-30.0 ± 0.3	-30.6 ± 1.1	-0.7 ± 1.1	1.01 ± 0.03
U-CR56W953S → RAPd3	$(1.22 \pm 0.19) \times 10^{-5}$	-28.0 ± 0.4	-45.2 ± 3.6	-17.2 ± 3.6	0.99 ± 0.04
U-CR56W953S → RAP	$(1.22 \pm 0.08) \times 10^{-5}$	-28.0 ± 0.2	-50.4 ± 2.9	-22.3 ± 2.9	1.15 ± 0.05

[a] Not applicable when no heat of binding is observed.

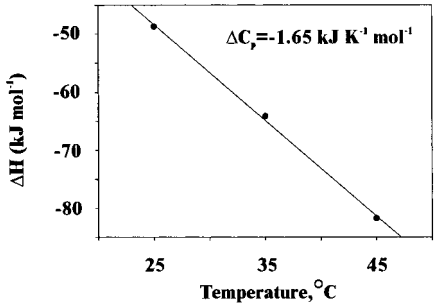

FIGURE 4: Plot of $\Delta H_b°$ vs T from the isothermal calorimetric titration of the formation of a complex of U-CR56 and RAPd1. A linear fit was made to estimate the heat capacity effect of complex formation, yielding a ΔC_p value of -1.65 kJ K^{-1} mol^{-1}. The correlation coefficient of the fit is 0.9985.

was found to have a much more favorable enthalpy of reaction with an entropy penalty, which was not observed for any of the other U-CR56 derivatives that were tested. In agreement with the failure of U-CR56W994S to bind RAPd3-coupled Sepharose (*44*), this CR-domain pair variant also did not exhibit any measurable binding in the ITC analysis. The calculated thermodynamic parameters are listed in Table 3. To substantiate the finding that the observed decrease in $\Delta H_b°$ for the binding of RAPd3 to U-CR56W953S is in fact significant, we also performed the reverse titration with U-CR56W953S (0.200 mM) in the stirring syringe and RAPd3 (0.0306 mM) in the sample cell. This experiment confirmed that the decrease in $\Delta H_b°$ for the association of RAPd3 with U-CR56W953S ($\Delta H_b° = -45.2$ kJ mol^{-1}) was nearly identical to the decrease described above.

The titration of U-CR56W953S (0.2062 mM) into RAP (0.0107 mM) (Figure 5A) showed an interaction with an affinity lower than that obtained in the corresponding experiment using U-CR56wt and, even more importantly, also demonstrated a less complex binding isotherm. Fitting the binding isotherm to a single set of binding sites showed that the thermodynamic parameters for such an interaction are similar in magnitude to those observed for the binding between U-CR56W953S and isolated RAPd3, suggesting that U-CR56W953S indeed is able only to associate with RAPd3 also in full-length RAP. However, we cannot exclude the alternative possibility of binding to other sites in RAP, but the data suggest that this mutant derivative will be of interest for further detailed binding analysis in clarifying the complex mechanism of binding between RAP and the receptor (fragments). A schematic data summary is presented in Figure 5B.

SPR Analysis of U-CR56 Binding to RAP and RAPd3. For further characterization of the interaction between U-CR56wt and RAP and RAPd3, we immobilized RAP and RAPd3 on a biosensor chip. The sensorgrams (Figure 6B) for U-CR56 binding to RAPd3 did not accurately fit a simple 1:1 langmuir binding isotherm, and since our calorimetric results might indicate the occurrence of a conformational change in RAPd3 upon formation of a complex with the receptor fragment, we fitted the sensorgrams using a two-state reaction mechanism involving a conformational change (eq 11). This resulted in accurate fitting using a simultaneous fit for the entire concentration series with an apparent K_D of 7.2×10^{-7} M. The accuracy of the fit for 1 μM U-CR56 together with the components of both the initially RAPd3·U-CR56 complex and the transformed complex is shown in Figure 6D. The same curve form was observed for the binding to immobilized RAP (Figure 6A), and as for the analysis for RAPd3, these sensorgrams could only be fitted accurately using the interaction model including a conformational change (Figure 6C). The fitting of RAP binding to only one site is suggestive of a negligible interaction between U-CR56 and RAPd1 of the immobilized full-length RAP, which suggests that RAPd1 is not ideal for immobilization using the amino coupling procedure. This is in accord with attempts to also use the BIAcore instrument for studying the binding to RAPd1, but after immobilization of RAPd1, we were

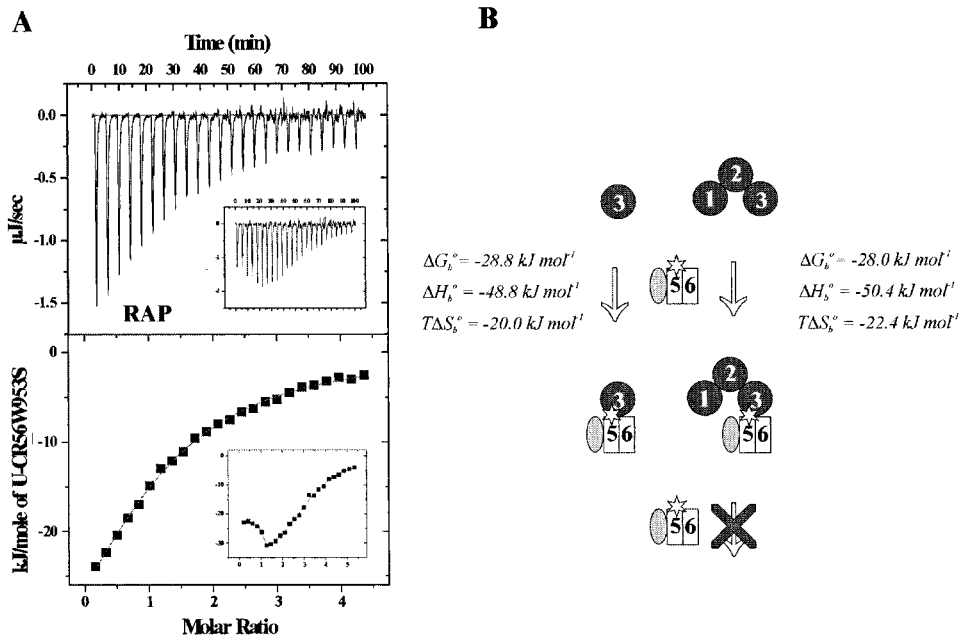

FIGURE 5: (A) Isothermal calorimetric titration analysis of association of full-length RAP with U-CR56W953S. Titration of RAP (0.0107 mM) with U-CR56W953S (0.2062 mM). The inset shows the corresponding titration with U-CR56wt into 0.00885 mM RAP for comparison (Figure 2C). (B) Schematic representation of the association between the mutated CR-domain pair U-CR56W953S and RAPd3, both in the isolated form and in full-length RAP. The thermodynamic parameters for the association between RAPd3 and U-CR56W953S are the mean values obtained from the reverse titration experiments (entries in Table 3). These values are very similar in magnitude to the parameters for the binding of U-CR56W953S to full-length RAP with an observed 1:1 stoichiometry (A), showing that only one molecule of this mutated CR-domain pair can associate with RAP, most likely via RAPd3.

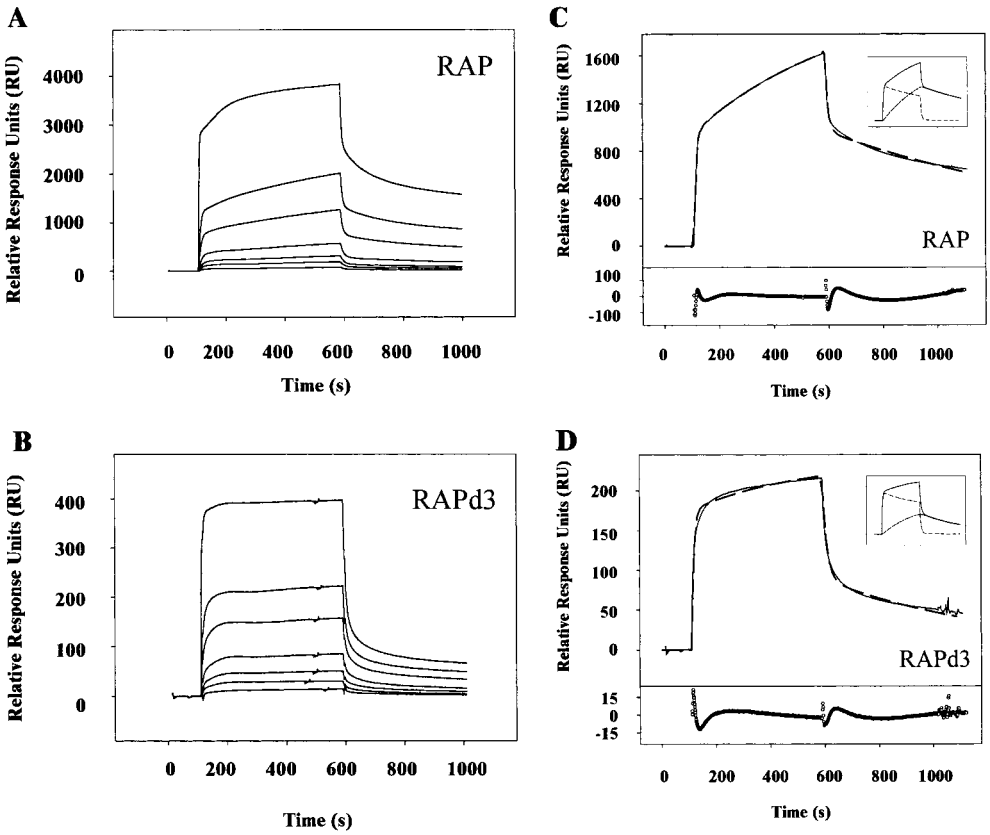

FIGURE 6: SPR analysis of U-CR56 binding to immobilized RAP and RAPd3. RAP (A) and RAPd3 (B) were immobilized on a biosensor chip at densities of 165 and 185 fmol/mm^2, respectively, and representative sensorgrams from the binding analysis of U-CR56 (20, 50, 100, 200, 500, 1000, and 5000 nM) are shown, where the plateau response in each sensorgram series corresponds directly to U-CR56 concentration. (C and D) Sensorgrams for 1 μM U-CR56 were fitted accurately using a two-state binding reaction involving a conformational change of RAPd3 (eq 12). The measured binding curve is shown as a solid line and the fitted curve using the model for a two-state reaction with a conformational change with a broken line. The inset shows the components of the encounter complex and transformed complex. Below are shown the residuals from the fitting procedure on a 10%-scaled axis.

Table 4: Kinetic Parameters Determined by SPR Analysis for the Interaction of RAP and RAPd3 with U-CR56wt at 25 °C

	RAP with U-CR56	RAPd3 with U-CR56
k_{a1} (M^{-1} s^{-1})	2.7×10^4	6.14×10^4
k_{d1} (s^{-1})	7.04×10^{-2}	7.76×10^{-2}
K_{A1} (M^{-1})	3.8×10^5	7.9×10^5
k_{a2} (s^{-1})	2.47×10^{-3}	1.02×10^{-3}
k_{d2} (s^{-1})	9.14×10^{-4}	1.33×10^{-3}
K_{A2}	2.7	0.77
K_A (M^{-1})	1.42×10^6	1.40×10^6
K_D (M)	7.0×10^{-7}	7.2×10^{-7}

unable to detect any binding of U-CR56. The kinetic parameters are given in Table 4.

DISCUSSION

We demonstrate that U-CR56wt can bind to three different binding sites in the full-length RAP molecule, with thermodynamic parameters nearly identical to those observed for the binding to each of the isolated RAP domains. This suggests that full-length RAP contains three independent receptor-binding units, most likely residing in RAPd1, RAPd2, and RAPd3, where the variation in the binding affinities suggests preferential binding of RAPd3 to CR-domain pairs as also demonstrated for full-length LRP (*30*).

The observed 1:1 stoichiometric binding between an isolated RAP domain and U-CR56wt suggests that only one RAP domain can bind to a tandem CR-domain pair. The significant decrease in affinity observed for mutation of residues located in both CR5 and CR6 further suggests that the binding site for a RAP domain is located at the interface between the two CR domains, and that high-affinity binding requires that two functionally CR domains be present.

The highly diverse binding thermodynamics for formation of a complex between U-CR56 and either RAPd1, RAPd2, or RAPd3 indicate different binding modes for RAPd1 and RAPd2 as opposed to RAPd3. A data summary is presented in Figure 3. The formation of a complex between U-CR56 and RAPd1 results in an entropy penalty that can be attributed to (1) ordering of the flexible linker between the CR domains upon binding, as also observed for the specific binding of the first three zinc fingers of the transcription factor TFIIIA with its cognate DNA sequence (*48*), or (2) ordering of the carboxyl-terminal part of RAPd1 upon binding since residues 92−112 do not have a well-defined conformation in the free RAPd1 (*49*). Indeed, we also tested a RAPd1 lacking residues 98−112, and observed a significant decrease in affinity for U-CR56wt. The ΔC_p for the binding reaction is small and is typical for binding interactions between proteins that do not involve significant gross conformational change (*50*). Whether the negative entropy is explained by a loss in degrees of freedom in the linker between the two CR domains, an ordering of the 20-residue carboxyl-terminal tail of RAPd1, or a combination of both can only be determined by further NMR analysis.

The affinity of binding of U-CR56 to RAPd2 is more than 100-fold lower than the affinity of binding to RAPd3, in accord with previously published LRP binding data (*28*, *30*), suggesting that this is not solely specific for the CR56-domain pair, but rather characteristic throughout the series of CR domains in the entire LRP receptor. We have previously shown that RAP fragments spanning both RAPd2 and either RAPd1 or RAPd3 are more potent inhibitors of RAP binding to LRP than RAPd1 and RAPd3 alone (*28*). We demonstrate here that these results are commensurate with the weak binding interaction observed between RAPd2 and U-CR56. Obermoeller and colleagues reported that a variant of RAPd2 (RAP residues 91−210) was able to partly inhibit the interaction of ^{125}I-labeled RAPd3 and α_2-macroglobulin with LRP on the cell surface, further demonstrating an interaction of the RAPd2 domain with LRP (*38*). However, a ^{125}I-labeled RAP fragment spanning residues 89−216 was shown not to bind LRP (*29*), but this is likely due to deleterious effects on the RAP domain by the oxidative radioiodination, a process found to destroy the receptor binding properties of RAPd1 (M. Etzerodt, unpublished observation).

The two sets of binding sites best describe the titration of U-CR56 into RAPd3 and would suggest binding to two RAPd3 species in solution. We propose that the high-affinity binding observed with the initial injections of U-CR56 is to a conformationally altered subpopulation of RAPd3 and that the $K_D \sim 10^{-7}$ M interaction involves a conformational change of this conformationally altered subpopulation upon binding. This is supported by analysis of the SPR data on the binding of U-CR56 to RAPd3, which is best described in terms of a two-state binding mechanism that yields a K_D of 7.2×10^{-7} M, a value fairly close to $\sim 10^{-7}$ M. NMR analysis indicates that a small portion of ^{15}N-labeled RAPd3 is folded, even in the absence of a receptor fragment (unpublished observations from O. Andersen and B. Kragelund, University of Copenhagen, Copenhagen, Denmark). Well-known examples of similar conformation changes are the binding of hirudin to thrombin (*51*), and the binding of the trp repressor to its target DNA (*52*). It is also in accord with the uncomplexed conformation of RAPd3 at pH 7.4 being dynamic as inferred from NMR analysis (*28*), and the fact that RAPd3 is the least structurally stable domain of the three RAP domains (*29*, *53*). The demonstration that the association of U-CR56wt with RAPd3 is accompanied by positive binding entropy suggests that RAPd3 may also be flexible in the bound state and that the binding may also involve disordering of the water structure in the bound state. An increase in the binding entropy is also observed for U-CR56wt binding to RAPd3 in the full-length RAP. This suggests that the stability of RAPd3 is not influenced by the rest of the RAP molecule (*29*), and could indeed explain the observed disordered structural signals from RAP in solution by NMR (unpublished). This flexibility of RAPd3 and the involvement of water in the binding mechanism may be linked to the functional properties of RAP as an escort protein in the secretory pathway, as RAPd3 is sufficient for mimicking the chaperone-like functions of full-length RAP (*38*, *54*).

The Trp residue was selected for mutation and binding analysis because residues at corresponding positions are suggested to be implicated in ligand interactions. A naturally occurring mutation converts an Arg residue at this position in the sixth CR domain in LDLR to a Trp residue which causes familial hypercholesterolemia (*13*), and the importance of the indole groups is further highlighted by the familial hypercholesterolemia that accompanies mutation of the Trp residue in the second CR domain of LDLR (*55*, *56*). The more favorable enthalpy but failure of entropic compensation for U-CR56W953S binding to RAPd3 indicates that either

(1) the Trp residues in the CR domains are critical for the flexibility of RAPd3 in the bound state or (2) the Trp residues are essential for the involvement of water in the binding interaction. The identification of only a single set of binding sites when U-CR56W953S was titrated into RAP with thermodynamic parameters similar to those for the association with RAPd3 is strongly suggestive of a model where binding between LRP and RAP is primarily mediated by the RAPd3 binding sites. The function of concurrent binding of RAPd1 and RAPd2 to other parts of the CR cluster may be stabilization of the interaction, as well as protecting a larger region of the potential ligand-binding region during ER processing. This hypothesis is in accord with the demonstration of RAPd1 as a potent inhibitor of α_2M binding to LRP, whereas RAPd3 is not (*28*, *57*). Furthermore, the possibility of trapping the interaction after the association of a single CR-domain pair with RAP could prove to be a very useful tool for the analysis of two remaining RAP domains with different CR-domain pairs. The observation that U-CR56R988Q binds RAPd3 with higher affinity than U-CR56 containing the wild-type sequence, as noted previously, was not unanticipated. This result suggests that an overall negative surface potential of a CR-domain pair will influence the recognition of ligands for the lipoprotein receptor family.

Finally, the fact that binding of RAPd3 is more dramatically affected by the mutation of residues in CR6 ($Trp994^{CR6}$ and $Asp999^{CR6}$) than the mutations of homologous residues in CR5 ($Trp953^{CR5}$ and $Asp958^{CR5}$) suggests that the CR-domain pair is an asymmetric binding unit, as expected for binding to RAPd3, another asymmetric binding unit. We have previously demonstrated the lack of RAPd3 binding to the CR-domain pair consisting of the two most carboxyl-terminal CR domains of LRP cluster II, CR9 and CR10, where CR10 is lacking both the Asp residue and the Trp residue (which are replaced with Asn and Lys residues, respectively) (*39*). It has also been demonstrated that neither RAP (*26*) nor RAPd3 (*38*) can bind to the CR-domain pair in LRP CR-cluster I (comprising CR1 and CR2), again where the carboxyl-terminal CR domain (CR2) contains Val and Arg residues instead of the Asp and Trp residues, respectively. This indicates that the binding of the most carboxyl-terminal CR domain of a CR-domain pair is a critical binding for RAPd3. However, high-affinity binding to the two adjoined CR domains only results in efficient binding to the amino-terminal CR domain of the pair as well. We suggest that this model for RAPd3 binding to a CR-domain pair can be extended to include the other RAPd3 binding CR-domain pairs in LRP CR cluster II, U-CR34, -45, -56, -67, -78, and -89 (*39*), since all six receptor fragments bind RAPd3 with similar affinities and the seven CR domains (CR3−CR9) all contain the Asp-Trp amino acid pair in their primary structure (*39*).

The binding of RAPd1 to the array of overlapping CR-domain pairs is more restricted (not shown), where the binding of RAPd1 to U-CR56 is in accord with previous reports showing that RAP residues 1−110 bind a fragment containing the amino-terminal flanking EGF domain and the four CR domains (CR3−CR6), whereas no binding was observed for the carboxyl-terminal part of LRP CR cluster II (*38*). The presence of three receptor-binding sites in RAP, as well as other CR-domain pairs in LRP CR cluster II which has the potential to bind RAP domains (*39*), suggests the possibility of multiple interactions for the binding of RAP to CR cluster II (schematically represented in Figure 7). The most likely binding is the association of RAPd3 with the site having the highest affinity toward RAPd3 (a). Depending on the flexibility of the three-domain RAP molecule, RAPd1 and/or RAPd2 may associate with other sites in the CR cluster, whereby the interaction involves concurrent binding to multiple RAP domains (b and c). Alternatively, the flexibility of the linkers between CR domains indicates that conformational transformations in the CR cluster may allow the CR domains to adopt a relative position optimal for different binding mechanisms (d and e). Finally, it cannot be concluded whether the proximity of RAPd1 to RAPd3 will favor binding of RAPd1 rather that RAPd3 from a second RAP molecule (f and g). Future studies must be carried out before it can be concluded that RAPd3 also binds more efficiently than the other two RAP domains to all CR-domain pairs.

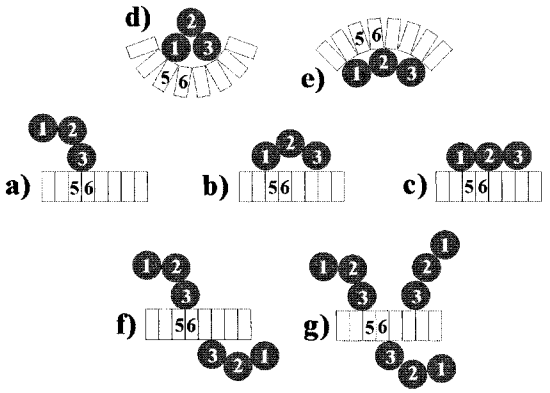

FIGURE 7: Putative model of multiple interaction possibilities between LRP CR cluster II and RAP domains. Illustration of concurrent binding via one, two, and three RAP domains to a single CR cluster (a−c, respectively). The binding of multiple CR-domain pairs to a single RAP molecule may have an allosteric effect resulting in the antagonization of the interaction of other ligands with the CR-cluster (d and e), which is also dependent on the number of sites which are occupied by RAP (domains). It may, alternatively, be more energetically favorable for multiple RAP molecules to coat the CR cluster via binding of RAPd3 to different CR-domain pairs (f and g).

ACKNOWLEDGMENT

We thank O. Lillelund, M. Madsen, and K. Sørensen for excellent technical assistance.

REFERENCES

1. Herz, J., Hamann, U., Rogne, S., Myklebost, O., Gausepohl, H., and Stanley, K. K. (1988) *EMBO J. 7*, 4119−4127.
2. Takahashi, S., Kawarabayasi, Y., Nakai, T., Sakai, J., and Yamamoto, T. (1992) *Proc. Natl. Acad. Sci. U.S.A. 89*, 9252−9256.
3. Kim, D.-H., Iijima, H., Goto, K., Sakai, J., Ishii, H., Kim, H.-J., Suzuki, H., Kondo, H., Saeki, S., and Yamamoto, T. (1996) *J. Biol. Chem. 271*, 8373−8380.
4. Yamazaki, H., Bujo, H., Kusunoki, J., Seimiya, K., Kanaki, T., Morisaki, N., Schneider, W. J., and Saito, Y. (1996) *J. Biol. Chem. 271*, 24761−24768.
5. Jacobsen, L., Madsen, P., Moestrup, S. K., Lund, A. H., Tommerup, N., Nykjær, A., Sottrup-Jensen, L., Gliemann, J., and Petersen, C. M. (1996) *J. Biol. Chem. 271*, 31379−31383.

6. Hey, P. J., Twells, R. C. J., Phillips, M. S., Yusuke, N., Brown, S. D., Kawaguchi, Y., Cox, R., Guochun, X., Dugan, V., Hammond, H., Metzker, M. L., Todd, J. A., and Hess, J. F. (1998) *Gene 216*, 103−111.
7. Kim, D.-H., Inagaki, Y., Suzuki, T., Ioka, R. X., Yoshioka, S. Z., Magoori, K., Kang, M.-J., Cho, Y., Nakano, A. Z., Liu, Q., Fujino, T., Suzuki, H., Sasano, H., and Yamamoto, T. T. (1998) *J. Biochem. 124*, 1072−1076.
8. Dong, Y., Lathrop, W., Weaver, D., Qiu, Q., Cini, J., Bertolini, D., and Chen, D. (1998) *Biochem. Biophys. Res. Commun. 251*, 784−790.
9. Brown, S. D., Twells, R. C. J., Hey, P. J., Cox, R. D., Levy, E. R., Soderman, A. R., Metzker, M. L., Caskey, C. T., Todd, J. A., and Hess, J. F. (1998) *Biochem. Biophys. Res. Commun. 248*, 879−888.
10. Daly, N. L., Scanlon, M. J., Djordjevic, J. T., Kroon, P. A., and Smith, R. (1995) *Proc. Natl. Acad. Sci. U.S.A. 92*, 6334−6338.
11. Daly, N. L., Djordjevic, J. T., Kroon, P. A., and Smith, R. (1995) *Biochemistry 34*, 14474−14481.
12. Fass, D., Blacklow, S., Kim, P. S., and Berger, J. M. (1997) *Nature 388*, 691−693.
13. North, C. L., and Blacklow, S. C. (2000) *Biochemistry 39*, 2564−2571.
14. Dolmer, K., Huang, W., and Gettins, P. G. W. (2000) *J. Biol. Chem. 275*, 3264−3269.
15. Huang, W., Dolmer, K., and Gettins, P. G. W. (1999) *J. Biol. Chem. 274*, 14130−14136.
16. Bieri, S., Atkins, A. R., Lee, H. T., Winzor, D. J., Smith, R., and Kroon, P. A. (1998) *Biochemistry 37*, 10994−11002.
17. North, C. L., and Blacklow, S. C. (1999) *Biochemistry 38*, 3926−3935.
18. North, C. L., and Blacklow, S. C. (2000) *Biochemistry 39*, 13127−13135.
19. Kurniawan, N. D., Atkins, A. R., Bieri, S., Brown, C. J., Brereton, I. M., Kroon, P. A., and Smith, R. (2000) *Protein Sci. 9*, 1282−1293.
20. Neels, J. G., Horn, I. R., van den Berg, B. M. M., Pannekoek, H., and van Zonneveld, A.-J. (1998) *Fibrinolysis Proteolysis 12*, 219−240.
21. Ashcom, J. D., Tiller, S. E., Dickerson, K., Cravens, J. L., Argraves, W. S., and Strickland, D. K. (1990) *J. Cell Biol. 110*, 1041−1048.
22. Strickland, D. K., Ashcom, J. D., Williams, S., Battey, F., Behre, E., McTigue, K., Battey, J. F., and Argraves, W. S. (1991) *J. Biol. Chem. 266*, 13364−13369.
23. Bu, G., Geuze, H. J., Strous, G. J., and Schwartz, A. L. (1995) *EMBO J. 14*, 2269−2280.
24. Willnow, T. E., Armstrong, S. A., Hammer, R. E., and Herz, J. (1995) *Proc. Natl. Acad. Sci. U.S.A. 92*, 4537−4541.
25. Willnow, T. E., Rohlmann, A., Horton, J., Otani, H., Braun, J. R., Hammer, R. E., and Herz, J. (1996) *EMBO J. 15*, 2632−2639.
26. Bu, G., and Rennke, S. (1996) *J. Biol. Chem. 271*, 22218−22224.
27. Warshawsky, I., Bu, G., and Schwartz, A. L. (1995) *Biochemistry 34*, 3404−3415.
28. Ellgaard, L., Holtet, T. L., Nielsen, P. R., Etzerodt, M., Gliemann, J., and Thøgersen, H. C. (1997) *Eur. J. Biochem. 244*, 544−551.
29. Medved, L. V., Migliorini, M., Mikhailenko, I., Barrientos, L. G., Llinás, M., and Strickland, D. K. (1999) *J. Biol. Chem. 274*, 717−727.
30. Tauris, J., Ellgaard, L., Jacobsen, C., Nielsen, M. S., Madsen, P., Thøgersen, H. C., Gliemann, J., Petersen, C. M., and Moestrup, S. K. (1998) *FEBS Lett. 429*, 27−30.
31. Bu, G., Williams, S., Strickland, D. K., and Schwartz, A. L. (1992) *Proc. Natl. Acad. Sci. U.S.A. 89*, 7427−7431.
32. Herz, J., Goldstein, J. L., Strickland, D. K., Ho, Y. K., and Brown, M. S. (1991) *J. Biol. Chem. 266*, 21232−21238.
33. Moestrup, S. K., and Gliemann, J. (1991) *J. Biol. Chem. 266*, 14011−14017.
34. Nykjær, A., Petersen, C. M., Møller, B., Jensen, P. H., Moestrup, S. K., Holtet, T. L., Etzerodt, M., Thøgersen, H. C., Munch, M., Andreasen, P. A., and Gliemann, J. (1992) *J. Biol. Chem. 267*, 14543−14546.
35. Orth, K., Madison, E. L., Gething, M.-J., Sambrook, J. F., and Herz, J. (1992) *Proc. Natl. Acad. Sci. U.S.A. 89*, 7422−7426.
36. Williams, S. E., Ashcom, J. D., Argraves, W. S., and Strickland, D. K. (1992) *J. Biol. Chem. 267*, 9035−9040.
37. Iadonato, S. P., Bu, G., Maksymovitch, E. A., and Schwartz, A. L. (1993) *Biochem. J. 296*, 867−875.
38. Obermoeller, L. M., Warshawsky, I., Wardell, M. R., and Bu, G. (1997) *J. Biol. Chem. 272*, 10761−10768.
39. Andersen, O. M., Christensen, L. L., Christensen, P. A., Sørensen, E. S., Jacobsen, C., Moestrup, S. K., Etzerodt, M., and Thøgersen, H. C. (2000) *J. Biol. Chem. 275*, 21017−21024.
40. Horn, I. R., van den Berg, B. M. M., van der Meijden, P. Z., Pannekoek, H., and van Zonneveld, A.-J. (1997) *J. Biol. Chem. 272*, 13608−13613.
41. Neels, J. G., van den Berg, B. M. M., Lookene, A., Olivecrona, G., Pannekoek, H., and van Zonneveld, A.-J. (1999) *J. Biol. Chem. 274*, 31305−31311.
42. Bu, G., and Schwartz, A. L. (1998) *Trends Cell Biol. 8*, 272−276.
43. Bu, G., and Paz Marzolo, M. (2000) *Trends Cardiovasc. Med. 10*, 148−155.
44. Andersen, O. M., Petersen, H. H., Jacobsen, C., Moestrup, S. K., Etzerodt, M., Andreasen, P. A., and Thøgersen, H. C. (2001) *Biochem. J. 357*, 289−296.
45. Wiseman, T., Williston, S., Brandts, J. F., and Lin, L. N. (1989) *Anal. Biochem. 179*, 131−137.
46. Lipschultz, C. A., Li, Y., and Smith-Gill, S. (2000) *Methods 20*, 310−318.
47. Sigurskjold, B. W., Berland, C. R., and Svensson, B. (1994) *Biochemistry 33*, 10191−10199.
48. Liggins, J. R., and Privalov, P. L. (2000) *Proteins Suppl.*, 50−62.
49. Nielsen, P. R., Ellgaard, L., Etzerodt, M., Thøgersen, H. C., and Poulsen, F. M. (1997) *Proc. Natl. Acad. Sci. U.S.A. 94*, 7521−7525.
50. Spolar, R. S., and Record, M. T., Jr. (1994) *Science 263*, 777−784.
51. Ayala, Y. M., Vindigni, A., Nayal, M., Spolar, R. S., Record, M. T., Jr., and Di Cera, E. (1995) *J. Mol. Biol. 253*, 787−798.
52. Ladbury, J. E., Wright, J. G., Sturtevant, J. M., and Sigler, P. B. (1994) *J. Mol. Biol. 238*, 669−681.
53. Rall, S. C. J., Ye, P., Bu, G., and Wardell, M. R. (1998) *J. Biol. Chem. 273*, 24152−24157.
54. Savonen, R., Obermoeller, L. M., Trausch-Azar, J. S., Schwartz, A. L., and Bu, G. (1999) *J. Biol. Chem. 274*, 25877−25882.
55. Jensen, H. K., Jensen, L. G., Hansen, P. S., Færgeman, O., and Gregersen, N. (1996) *Atherosclerosis 120*, 57−65.
56. Moorjani, S., Roy, M., Torres, A., Bétard, C., Gagné, C., Lambert, M., Brun, D., Davignon, J., and Lupien, P. (1993) *Lancet 341*, 1303−1306.
57. Bu, G., Maksymovitch, E. A., Geuze, H., and Schwartz, A. L. (1994) *J. Biol. Chem. 269*, 29874−29882.

BI0110692